HHS Public Access

Author manuscript

Clin Cancer Res. Author manuscript; available in PMC 2016 August 01.

Published in final edited form as:

Clin Cancer Res. 2015 August 1; 21(15): 3561–3568. doi:10.1158/1078-0432.CCR-14-1051.

Desmoplasia in primary tumors and metastatic lesions of pancreatic cancer

Clifford J. Whatcott[1,†], **Caroline H. Diep**[1], **Ping Jiang**[2], **Aprill Watanabe**[3], **Janine LoBello**[3], **Chao Sima**[4], **Galen Hostetter**[5], **H. Michael Shepard**[2], **Daniel D. Von Hoff**[1], and **Haiyong Han**[1,†]

[1]Clinical Translational Research Division, The Translational Genomics Research Institute, Phoenix, Arizona, 85004

[2]Halozyme Therapeutics, San Diego, CA, 92121

[3]Integrated Cancer Genomics Division, The Translational Genomics Research Institute, Phoenix, Arizona, 85004

[4]Computational Biology Division, The Translational Genomics Research Institute, Phoenix, Arizona, 85004

[5]Laboratory of Analytical Pathology, The Van Andel Research Institute, Grand Rapids, MI, 49503

Abstract

Purpose—Pancreatic ductal adenocarcinoma (PDAC) is characterized by high levels of fibrosis, termed desmoplasia, which is thought to hamper the efficacy of therapeutics treating PDAC. Our primary focus was to evaluate differences in the extent of desmoplasia in primary tumors and metastatic lesions. As metastatic burden is a primary cause for mortality in PDAC, the extent of desmoplasia in metastases may help to determine whether desmoplasia targeting therapeutics will benefit patients with late stage, metastatic disease.

Experimental Design—We sought to assess desmoplasia in metastatic lesions of PDAC and compare it to that of primary tumors. Fifty three patients' primaries and fifty seven patients' metastases were stained using immunohistochemical staining techniques.

Results—We observed a significant negative correlation between patient survival and extracellular matrix deposition in primary tumors. Kaplan-meier curves for Collagen I showed median survival of 14.6 months in low collagen patients, and 6.4 months in high level patients (log rank, $P<0.05$). Low level hyaluronan patients displayed median survival times of 24.3 months as compared to 9.3 months in high level patients (log rank, $P<0.05$). Our analysis also indicated that

[†]Correspondence: CJW, 445 North Fifth Street, Suite 400, Phoenix, AZ 85004, cwhatcott@tgen.org, Ph: 602-343-8631, Fax: 602-343-8740. HH, 445 North Fifth Street, Suite 400, Phoenix, AZ 85004, hhan@tgen.org, Ph: 602-343-8739, Fax: 602-343-8440.

Authors' contributions

Concept and design: CJW, DDVH, HH. Methodology: CJW, CHD, PJ, AW, JL, GH, HMS. Data acquisition (e.g., acquisition of samples, provided immunostaining protocols, etc.): CHD, PJ, AW, JL. Data analysis (e.g., statistical analysis): CJW, CS, DDVH, HH. Writing, review, and/or revision of the manuscript: CJW, CHD, PJ, AW, JL, CS, GH, HMS, DDVH, HH. All authors read and approved the final manuscript.

Potential conflict: PJ and HMS are employees of Halozyme Therapeutics. DDVH receives research support from Halozyme Therapeutics.

extracellular matrix components, such as collagen and hyaluronan, are found in high levels in both primary tumors and metastatic lesions. The difference in the level of desmoplasia between primary tumors and metastatic lesions was not statistically significant.

Conclusion—Our results suggest that both primary tumors and metastases of PDAC have highly fibrotic stroma. Thus, stromal targeting agents have the potential to benefit PDAC patients, even those with metastatic disease.

Keywords

tumor microenvironment; extracellular matrix; pancreatic cancer; metastasis

Introduction

Pancreatic ductal adenocarcinoma (PDAC) is the fourth leading cause of cancer-related death in the United States. With the 5-year survival rate at approximately 6%, novel therapeutic strategies are desperately needed to enhance patient outcomes (1). PDAC is characterized by the development of extensive fibrosis at primary tumor sites (2). This fibrosis is termed desmoplasia. In normal tissues, mechanisms common to desmoplasia may serve to aid in inflammation and resolution of granulation tissue in the wound healing process. However, in tumor tissues such as in PDAC, desmoplasia promotes tumor development and inhibits drug penetration and uptake (3, 4). Metastatic disease burden, on the other hand, is one of the primary causes of death in patients with PDAC. Metastatic lesions disrupt organ function, leading to hepatic failure, for example, when pancreatic metastases colonize the liver (5, 6). Recent reports have suggested that targeting components of the desmoplastic reaction may enhance the activity of therapeutics targeting tumor cells (7–11). The concern remains, however, of whether desmoplasia-targeting therapeutics will offer clinical benefit for patients with metastatic disease. To this end, we sought to determine the impact of desmoplasia on patient outcomes. In this report, we also sought to determine if metastatic lesions of PDAC are desmoplastic. To assess the extent of desmoplasia in these tissues, we looked at the expression of multiple extracellular matrix components and proteins, as well as cellular morphology in tissues taken from a diversity of patients. To our knowledge, this is the first report on the desmoplastic nature of pancreatic metastases to various sites.

In desmoplasia, the pancreatic stellate cell (PSC) transforms from a quiescent, lipid droplet-storing cell to that of an activated, smooth muscle actin expressing cell via Transforming growth factor β (TGFβ) and Platelet-derived growth factor (PDGF)-mediated transcriptional programs, eliciting ECM synthesis and deposition (12, 13). TGFβ plays a key role in this activation through both autocrine and paracrine signaling mechanisms (14). Reports have suggested that PSC activation and deposition of ECMs leads to increases in both tissue solid stress and tissue interstitial fluid pressures, both of which may mediate vascular compression and dysfunction (8, 15). Expansion of the stromal compartment and ECM deposition are thought to result in the poor drug penetration observed in PDAC. Indeed, Olive and colleagues observed marked decreases in the delivery of doxorubicin to tumor tissues in a genetically engineered mouse model (KPC) for pancreatic cancer, relative to adjacent normal tissues (16). Stromal expansion is accompanied by significant tissue hypovascularity

– with as much as a 75% decrease in tissue vessel density – observed in both KPC tumor and human tumor tissue sections (16). The combination of these factors reduces both the capability and availability of drug penetration in PDAC. Desmoplasia is well documented in the pathogenesis of primary tumors of PDAC. However, metastatic burden is also considered a major cause of patient death (17).

Metastatic disease burden results in organ failure and patient death. In a study of over five hundred autopsies performed at Roswell Park Memorial Institute of patients who had succumbed to various cancer types, organ invasion resulting in organ failure was found in 15% of patients (18). In a subsequent study, hepatic failure resulting in patient death was associated with primary tumors in the pancreas (6). Systemic delivery of chemotherapeutics attempts to redress metastatic disease burden both in the palliative and the neoadjuvant settings. It is not altogether obvious, however, whether metastatic lesions are also desmoplastic, and thus physiologically chemoresistant. Duda and colleagues suggest that malignant cells facilitate colonization of new tissues by conscripting activated fibroblasts, tending the notion that metastatic lesions may be desmoplastic (19). Consistent with the notion that desmoplasia inhibits drug uptake in primary tumors of the pancreas, desmoplastic metastases then would also be expected to be resistant to drug uptake by virtue of this same mechanism. If so, it is important that we understand the nature of desmoplasia in metastatic lesions if we are to enhance patient outcomes.

Recent reports suggest that concomitant stromal targeting may enhance therapeutic outcomes in PDAC patients. In the present study, we observed a negative correlation between patient survival and components of the ECM. In addition, we found similar levels of fibrosis in metastatic lesions compared to unmatched tumor primaries, as assessed by tissue levels of ECM components. We therefore conclude that stromal targeting approaches may also be beneficial to patients with metastatic disease. These findings suggest that research in stromal targeting may yield added therapeutic benefit in PDAC patients.

Materials and Methods

Case selection

Pancreatic ductal adenocarcinoma tumor samples were obtained from formalin-fixed and paraffin-embedded (FFPE) tissue blocks collected for clinical purposes between the years 1999 and 2009 at Scottsdale Healthcare (Scottsdale, AZ). Tumor data regarding histological subtype, grade, and TNM classification were obtained from de-identified pathology reports. Demographic information, such as age at diagnosis, gender, histology, stage of disease, smoking history, and overall survival (OS) were also noted from de-identified, retained records at Scottsdale Healthcare. The PDAC diagnosis, histological subtype, and TNM staging was determined by a board-certified staff pathologist at Scottsdale Healthcare. In addition histomorphologic confirmation was made by a second board-certified pathologist at TGen (GH). Additional patient-matched primary and metastasis samples were obtained from Yonsei University, Cancer Metastasis Research Center (Seoul, South Korea) for use in this report. The PDAC diagnosis was confirmed on these samples at Yonsei University by a staff pathologist prior to use in study.

Tissue microarray construction

Tissue microarrays (TMA) were constructed with 1 mm diameter cores punched from two to three distinct regions of each FFPE tumor block, compiled from both primary tumors and metastatic lesions (43 samples are represented with 3 cores, and 7 samples are represented with 2 cores). Tumor regions to be sampled were reviewed by study pathologist (GH) and TMA construction was performed using a Veridiam Semi-Automated Tissue Arrayer (VTA-100).

Immunohistochemical staining and assessment

TMA blocks were sectioned at 5μm and attached to Fisherbrand Superfrost® plus slides (Fisher Scientific) by water flotation and overnight drying. Slides were subsequently deparaffinized with xylene, rehydrated through a series of graded ethanol baths and antigen retrieved on-line using a BondMax™ autostainer (Leica Microsystems, Bannockburn, IL). All antibodies used in this study were obtained from Abcam (Cambridge, MA). Slides were visualized using either the Bond™ Polymer Refine Detection kit (Leica) using 3,3′-diaminobenzidine tetrahydrochloride chromogen as substrate or 4plus goat anti-mouse IgG biotinylated secondary antibody (Biocare Medical) using 3,3′-diaminobenzidine tetrahydrochloride chromogen as substrate. Percent area scoring was performed using Adobe Photoshop software (Adobe Systems, San Jose, CA). Slides were digitally scanned using an Aperio Scanscope (Leica Microsystems) and imported into Photoshop. Images were then converted to a CYMK color format, and the yellow channel was assessed for its intensity in monochrome grayscale. Assessment of the yellow channel allowed for quantitation of the development of brown chromogen on our slides, without also inadvertently measuring blue or red coloring. A threshold was selected and used which identified positive pixels on our slides. Percent area was calculated as a percentage of positive pixels relative to the total number of pixels in view. Staining intensity was assessed independently by two of the authors (CJW and HH) upon review of multiple random snapshots taken from the digitally scanned slides. Hyaluronan (HA) and Collagen I (Col I) staining was assessed by use of a combination score, where percent area was multiplied by the intensity of the stain, for a maximum possible score of 300. This combination score was used as a surrogate readout of the extent of fibrosis, where indicated by HA and Col I positivity. Patients with ‘low HA’ were defined where tissues exhibited a total HA histochemical score of 112 or less. ‘High HA’ patient samples were defined where total HA histochemical staining was 113 or greater. Patients with ‘high Col I’ had a total 185 or greater immunohistochemical score, based on multiple images taken from FFPE slides. ‘Low Col I’ was defined as patients with a total 184 or lower immunohistochemical score. Total combination cutoff scores for both HA and Col I were selected following Receiver-Operator Characteristic (ROC) Curve analysis (20). Total scores yielding the highest area under the curve (AUC) with ROC analysis were used as the cutoff for the survival curves. ROC analysis in our cohort yielded AUC for HA and Col I of 0.75 and 0.70, respectively. Total scores used to separate low and high groups for α-SMA, Col III, and Col IV, were 77, 128, and 53, respectively. ROC analysis yielded AUC for α-SMA, Col III, and Col IV of 0.59, 0.79, and 0.68, respectively.

Pentachrome staining was achieved by following the manufacturer’s protocol (American Master Tech, Lodi, CA). Briefly, slides were first deparaffinized with xylene, rehydrated

through a series of graded ethanol baths, and stained with Verhoeff's Elastic Stain. Following rinsing and differentiation steps, slides were placed in glacial acetic acid, and then in a 1% Alcian Blue solution. Following similar rinsing procedures, slides were also exposed to Crocein Scarlet – Acid Fuchsin, 5% Phosphotungstic Acid, and an Alcoholic Saffron Solution.

Hyaluronan staining was achieved using the hyaluronan binding protein (HABP) as has been described previously (21). Briefly, sections were deparaffinized, followed by rehydration. Slides were first incubated with an avidin and biotin solution and then placed in a 0.3% hydrogen peroxide, diluted in methanol. Slides were then incubated with 1% bovine serum albumin as a blocking solution and detected using biotinylated HABP (2μg/mL) on our autostainer. After washing with PBS, HRP-streptavidin was applied at room temperature. Slides were then visualized using diaminobenzidine tetrahydrochloride treatment. Hyaluronan-specific staining was confirmed using recombinant human hyaluronidase (Halozyme Therapeutics, San Diego, CA) pre-treatment prior to the above protocol on control slides.

Statistical Analysis

Survival and immunohistochemical staining data were analyzed using GraphPad Prism 5 software (GraphPad Software, La Jolla, CA). Survival data are presented in Kaplan-Meier curves, in which the statistical significance of the median survival times was assessed using a Log-rank test. Statistical significance in our immunohistochemical data was analyzed with a standard, unpaired t test. Cox regression analyses were performed using R, version 3.0.1, on clinical data to assess significance of the correlation between pathologic parameters and patient survival. Univariate analysis was followed by multivariate analysis where we assessed the statistical significance of our observations, adjusting for the confounding influence of these clinicopathologic factors on tissue staining, by first selecting parameters which had met a threshold P value of less than 0.2. Parameters which had met this threshold were analyzed using multivariate Cox regression analysis. P values of less than 0.05 were considered significant.

Results

Components of the extracellular matrix and their correlation with survival in pancreatic cancer patients

Considering recent reports on the impact of HA in the chemoresistance of tumors in KPC mice, we evaluated HA and other ECMs in a cohort of human patient samples (8, 22). We sought to determine if any correlation existed between ECM deposition and patient survival. A total of 50 patients with pathologic diagnoses of pancreatic ductal adenocarcinoma and with survival data were identified and included in this study. Median age of the patients included was 69 years, with male and female individuals comprising 52% and 48% of the cohort, respectively. Patients included were predominantly of Caucasian race. These and other demographic data are summarized online (Supplementary Table S1). TNM staging and overall survival ranges are shown as well (Supplementary Table S2). Median survival for all patients was 13.3 months. Individual patient follow-up was maintained for over 100 months.

In analyses of correlation between survival and other clinicopathalogical parameters by Cox regression analysis, statistical significance was identified with lymph node status and combined AJCC staging status (Col I and Col IV), as well as well as age and combined AJCC staging status (HA). No statistically significant correlation was observed between survival and gender, smoking status, or histological grading (Supplementary Table S3). It should be noted that significant correlations have been observed in prior studies with lymph node status and patient survival (23). Further, full treatment history was not available for analysis in this context. Multivariate analyses were also performed on IHC staining and other clinicopathological parameters versus survival. As shown in Supplementary Table S4, Col I, Col IV, and HA retain a significant association with survival (P=0.015, 0.034, and 0.033, respectively).

To quantify the tissue staining of HA and Collagen I in the primary tumors of patients, we analyzed tissue sections according to percent area staining as well as staining intensity (24). The survival curves of the high and low HA also demonstrated a statistically significant difference (log rank, P=0.037) with a calculated hazard ratio of 2.6. The difference in median survival between the high and low HA curves was 15.0 months. Curves were statistically compared using a Log-rank test, demonstrating that the curves for high and low Col I (P=0.013) were statistically different, with a calculated hazard ratio of 2.3, for higher levels of Col I. The difference in median survival between the high and low Col I curves was 8.2 months. Kaplan-Meier curves displaying overall survival based on the expression of HA and Col I are shown in Figure 1. For comparison, survival analysis for α-smooth muscle actin (α-SMA, a marker for myofibroblasts), Col III, or Col IV is also shown in Supplementary Figure S1. Patients whose tumors have high α-SMA or Col III did not exhibit statistically significant correlations toward shorter survival (P=0.97 and 0.09 for a-SMA and Col III, respectively) (Supplementary Figure S1). A statistically significant difference between high and low Col IV patient groups was observed (P<0.05). Because of the negative correlations that we observed, we decided to expand our analysis and subsequently evaluated markers of desmoplasia histochemically in both primary tumors and metastatic lesions.

Desmoplastic features in primary tumors and metastatic lesions

The desmoplasia and dense extracellular matrix of PDAC primary tumors has been well documented (2). To compare the desmoplastic features between primary and metastatic lesions, we first stained the tissues with Movat's pentachrome stain. Movat's pentachrome staining, which was originally developed to stain connective tissue, indicates the presence of collagens in yellow. As can be seen in Figure 2, except for small areas of interlobular staining, the yellow collagen staining was largely absent in adjacent normal tissues (Figure 2, pentachrome stain). On the contrary, intense collagen staining was observed throughout primary tumor tissues. H&E staining shows acinar microarchitecture loss accompanied by basement membrane degradation and escape of neoplastic cells from ductal compartments in the primary tumor. Individual tumor glands are surrounded by dense stromal cells, which correspond to intense and diffuse collagen expression in the pentachrome staining, consistent with the notion that stromal cells are responsible for the production of collagens. Intriguingly, the liver metastasis also showed significant quantities of stromal cells (Figure

2, H&E, Metastasis). This stromal cell population also corresponded to increased collagen expression, as indicated in pentachrome stained section. This observation indicates that PDAC metastases are also desmoplastic, and appear to be very similar in the extent to that of the primary tumor. To further examine desmoplasia in PDAC metastases and primary tumors, we next evaluated additional markers of desmoplasia.

Levels of extracellular matrix components in both primary tumors and metastatic lesions

Activated stellate cells (or myofibroblasts) are the primary source of ECMs in pancreatic desmoplasia (25). We stained tissue sections with α-SMA and cytokeratin (an epithelial cell marker) to distinguish cell types. As shown in Figure 2, acinar and epithelial cells stained strongly for cytokeratins in all three tissue locations, adjacent normal, primary tumor, and liver metastases. PSCs and other stromal cells did not stain for cytokeratin. α-SMA staining was not observed in acinar or epithelial cells, but was observed in a majority of the stromal cells of primary tumors and metastases (Figure 2, α-SMA). Similar to that seen in H&E staining, the tumor glandular structures are interwoven with α-SMA positive stromal cells. Next, we sought to examine the expression levels of individual major ECM components. We stained a tumor TMA containing one hundred and seven evaluable and unique patient primary tumors and metastases sections, with antibodies specific to collagen I, III, IV, and HA. Figure 3 shows the representative images of the ECM proteins in PDAC tissues. For collagen I, we observed significantly stronger staining in the stromal compartment of both tumor and metastases (Figure 3, Collagen I). Adjacent normal tissues appeared to express collagen I in the peri-acinar cell space. For collagen III, we observed similar staining patterns in tumor and liver tissues to that seen with collagen I. However, staining in adjacent normal tissues appeared to be limited to the peri-lobular space. The staining patterns and intensity of collagen IV and HA were similar to those of collagen I.

To assess what differences, if any, exist in the desmoplastic reaction between primary tumors and metastatic lesions, we first sought to compare collagen I expression in patient matched samples from both sites (representative images shown in Figure 4). In a small set of seven patients, we saw comparable levels of collagen I expressed in both primary tumors and in tissues excised from the corresponding metastases. For further analysis we next sought to measure Collagen I expression in our TMA data sets. For quantitation, we assessed Collagen I staining by percentage area where positive staining occurred. Using unmatched primary tumors and metastatic lesions from our TMA, we measured the percentage area in which Collagen I stained positively in a given snapshot of a tumor section. All metastatic sites were pooled, and compared to the percentage positive staining observed in pooled primary tumors. The percentage area was assessed from multiple images of each patient tumor by two independent observers. Figure 4 (right panel) shows the distribution of the percentage area of positive Col I staining in all primary and metastasis cases. The average percentage area for the primary tumor cases is 74.0 and the average percentage area for the metastasis cases is 68.0. There is no statistically significant difference in percentage area between the two groups. Col III, Col IV, HA, and α-SMA staining was also assessed in a similar fashion (Supplementary Figure S2). Like Col I, Col III levels were not different in the metastatic lesions when compared to primary tumors (64.5 vs. 58.9, n.s.). Col IV, HA, and α-SMA, however, were found to be present at

comparable, though statistically different, levels in primary tumors versus metastatic lesions (42.4 vs. 33.9, 78.2 vs. 69.5, and 42.9 vs. 49.8, respectively). These results indicate that in PDAC the metastatic lesions have similar levels of the desmoplastic reaction to those of primary tumors.

Discussion

In our efforts to understand the role of the stroma in cancer, we have endeavored to determine whether stromal targeting therapy has the potential to increase patient survival in pancreatic cancer. However, one lingering concern has been a limited understanding of desmoplasia in metastatic lesions. Indeed, 'will stroma targeting therapy have any effect in late stage, metastatic disease if metastatic lesions are not also desmoplastic?' To begin to address these concerns, in this study, we sought to answer the question, 'what role, if any, does desmoplasia play in the outcomes of patients with pancreatic cancer?' Our results demonstrate that ECMs such as hyaluronan and collagen, surrogates for desmoplastic activity, correlate negatively with patient survival. Also, our findings show that there is no significant difference between the extent of desmoplasia in primary tumors and metastatic lesions.

To the question, "does the presence of desmoplastic ECMs correlate with poor survival in pancreatic cancer," our data demonstrated that survival correlated negatively with the amount of hyaluronan in tumors. Hyaluronan is a linear polysaccharide that plays an important role in a range of cellular processes. Hyaluronan related signaling pathways (including CD44-mediated) are thought to be involved in biological functions including cell proliferation, tissue hydration, cell motility, inflammation, angiogenesis, and malignancy. Increases in hyaluronan levels have been observed in many different cancer types, including pancreatic, breast, gastric, and bladder cancer (26–29). As hyaluronan can act as a molecular sieve, enhancing residence time and reducing penetration of macromolecules, we hypothesized that the levels of ECMs like hyaluronan correlate with survival in pancreatic cancer. Hyaluronan binding protein (HABP) interrogation of hyaluronan levels yielded histochemical images of rather uniform staining intensities. We assessed patient tissues using positive staining area in a given image as a measure of the synthesis of hyaluronan. Here also, hyaluronan staining served in large part as a surrogate stain for the extent of desmoplasia in our tissue samples. Because of its increased levels in cancer, however, hyaluronan has already been proposed as a suitable drug target (30). Indeed, interventions are under current investigation for targeting stromal components like hyaluronan (clinicaltrials.gov, NCT01839487).

In addition to hyaluronan, Collagens I, III, and IV are expressed at high levels in pancreatic cancer. Receptor signaling mechanisms mediated by integrin subunits have been shown to be dysregulated. Though the subunit expression trends are not altogether clear, integrin receptor combinations such as $\alpha_v\beta_3$, $\alpha_v\beta_6$, and $\alpha_6\beta_4$, have been shown to enhance proliferation and tumorigenesis (31–33). But as with hyaluronan, collagen levels are thought to negatively correlate with penetration of macromolecules into tumor tissues as well. We hypothesized and interrogated collagen I for correlations with patient survival. In a prior report, Erkan and colleagues found a positive correlation with collagen levels and patient

survival (24). One possible explanation for this discrepancy between our findings may be found in the different staining methods that were used for collagen. Erkan *et al* used the amphoteric dye, aniline blue, whereas we used collagen I specific immunostaining. Non-specific for the collagen subtypes, their data suggests, taken together with our findings, that additional alterations in other collagen subtypes may be occurring. Indeed, it may suggest significant loss of other collagen subtypes to account for the overall loss Erkan and colleagues observed in association with the poorly surviving cohort. An additional explanation for the discrepancy might also be found in prior treatments the patients received, resulting in overall changes in collagen deposition. Further investigation will be needed to make this determination.

To the question, “are metastatic lesions also desmoplastic,” our findings suggest that primary tumors and metastatic lesions both show significant levels of desmoplasia (Figure 4). Our data suggest that metastatic lesions of multiple sites, including liver, lung, and the peritoneal cavity, display significant and comparable levels of desmoplasia, including high levels of collagens I, III, and IV, to that found in primary pancreatic tumors (Figure 4, right panel). While expanded cohorts of each metastatic site are needed to confirm the organ site-specific consequences of fibrosis, we have observed that together, the metastatic lesions are statistically indistinguishable in their percent area of fibrosis, as measured by Collagen I, from primary pancreatic tumors regardless of metastatic site (Table 1). Indeed, our small sample of matched pairs of patient tumors supports these findings (Figure 4, Table 2). Since we do not have detailed treatment history from our patient cohort, it is possible that prior treatment could potentially bias the results as reported. Nonetheless, our data suggest that ECM *retention* in the context of chemotherapeutic treatment correlates negatively with patient survival for HA, Col I, and Col IV. Together with studies showing negative correlation between collagen levels and macromolecule penetration, these findings suggest that patients with metastatic disease may potentially benefit from stroma targeting therapies (34). The origin of demosplasia-inducing myofibroblasts in metastatic lesions is debated, but appears to originate from the primary tumor in some models (19). In the liver, where pancreatic cancer cells commonly metastasize, desmoplasia is also recognized as a physiological response to tumors arising *in situ*. Whether myofibroblasts are brought to the site of metastasis, or whether they are resident myofibroblasts of the liver, significant desmoplasia in metastatic lesions suggest that metastasizing tumors maintain pre-established intercellular signaling mechanisms with stromal cells post-metastasis.

It is clear from prior studies that PDAC patients may die from metastatic disease burden and subsequent organ failure (6, 17, 35). Are stromal targeted therapies expected to have a therapeutic benefit in metastatic disease? Or, would they instead only be expected to be effective where the primary tumor is known to be desmoplastic? Recent studies have pointed to the tumor microenvironment as a potential area by which to achieve greater patient outcomes via chemotherapeutics. By targeting tumor-stromal interactions, the hope has been to enhance current regimens, or to identify new potential strategies. It is clear that stromal interactions promote primary tumor growth and pathogenesis. The current study demonstrates that metastatic lesions, too, are desmoplastic, suggesting that patients with metastatic disease may also benefit from stromal targeted therapies.

Supplementary Material

Refer to Web version on PubMed Central for supplementary material.

Acknowledgments

This work is supported by a Stand Up to Cancer Translational Research Grant, a Program of the Entertainment Industry Foundation administered by the American Association for Cancer Research (SUC2-AACR-DT0509). This work was also supported in part by R01 (CA169281) and U01 (CA128454) grants from the NIH/NCI, by financial contributions from the Katz Family Foundation, and by a grant from the National Foundation for Cancer Research (NFCR).

We thank Dr. Sun Young Rha, Chief of the Division of Genomics and Translational Research, Cancer Metastasis Research Center, at Yonsei University, and her team, for their assistance and contribution of tissue samples for our study. We would also like to thank Amol Tembe at TGen, and Sha Tao at the Van Andel Research Institute, for their assistance in the statistical analysis of our data.

References

1. Siegel R, Ma J, Zou Z, Jemal A. Cancer statistics. CA Cancer J Clin. 2014; 64:9–29. [PubMed: 24399786]
2. Mahadevan D, Von Hoff DD. Tumor-stroma interactions in pancreatic ductal adenocarcinoma. Mol Cancer Ther. 2007; 6:1186–97. [PubMed: 17406031]
3. Minchinton AI, Tannock IF. Drug penetration in solid tumours. Nat Rev Cancer. 2006; 6:583–92. [PubMed: 16862189]
4. Netti PA, Berk DA, Swartz MA, Grodzinsky AJ, Jain RK. Role of extracellular matrix assembly in interstitial transport in solid tumors. Cancer Res. 2000; 60:2497–03. [PubMed: 10811131]
5. Chiang AC, Massague J. Molecular basis of metastasis. N Engl J Med. 2008; 359:2814–23. [PubMed: 19109576]
6. Houten L, Reilley AA. An investigation of the cause of death from cancer. J Surg Oncol. 1980; 13:111–16. [PubMed: 7359917]
7. Neesse A, Frese KK, Bapiro TE, Nakagawa T, Sternlicht MD, Seeley TW, et al. CTGF antagonism with mAb FG-3019 enhances chemotherapy response without increasing drug delivery in murine ductal pancreas cancer. Proc Natl Acad Sci U S A. 110:12325–30. [PubMed: 23836645]
8. Provenzano PP, Cuevas C, Chang AE, Goel VK, Von Hoff DD, Hingorani SR. Enzymatic targeting of the stroma ablates physical barriers to treatment of pancreatic ductal adenocarcinoma. Cancer Cell. 2012; 21:418–29. [PubMed: 22439937]
9. Von Hoff DD, Ramanathan RK, Borad MJ, Laheru DA, Smith LS, Wood TE, et al. Gemcitabine plus nab-paclitaxel is an active regimen in patients with advanced pancreatic cancer: a phase I/II trial. J Clin Oncol. 29:4548–54. [PubMed: 21969517]
10. Jain RK. Normalizing tumor microenvironment to treat cancer: bench to bedside to biomarkers. J Clin Oncol. 31:2205–18. [PubMed: 23669226]
11. Von Hoff DD, Ervin T, Arena FP, Chiorean EG, Infante J, Moore M, et al. Increased survival in pancreatic cancer with nab-paclitaxel plus gemcitabine. N Engl J Med. 2013; 369:1691–03. [PubMed: 24131140]
12. Yen TW, Aardal NP, Bronner MP, Thorning DR, Savard CE, Lee SP, et al. Myofibroblasts are responsible for the desmoplastic reaction surrounding human pancreatic carcinomas. Surgery. 2002; 131:129–34. [PubMed: 11854689]
13. Faouzi S, Le Bail B, Neaud V, Boussarie L, Saric J, Bioulac-Sage P, et al. Myofibroblasts are responsible for collagen synthesis in the stroma of human hepatocellular carcinoma: an in vivo and in vitro study. J Hepatol. 1999; 30:275–84. [PubMed: 10068108]
14. Akhurst RJ, Hata A. Targeting the TGFbeta signalling pathway in disease. Nat Rev Drug Discov. 11:790–11. [PubMed: 23000686]

15. Stylianopoulos T, Martin JD, Chauhan VP, Jain SR, Diop-Frimpong B, Bardeesy N, et al. Causes, consequences, and remedies for growth-induced solid stress in murine and human tumors. Proc Natl Acad Sci U S A;. 109:15101–08.
16. Olive KP, Jacobetz MA, Davidson CJ, Gopinathan A, McIntyre D, Honess D, et al. Inhibition of Hedgehog signaling enhances delivery of chemotherapy in a mouse model of pancreatic cancer. Science. 2009; 324:1457–61. [PubMed: 19460966]
17. Yachida S, Jones S, Bozic I, Antal T, Leary R, Fu B, et al. Distant metastasis occurs late during the genetic evolution of pancreatic cancer. Nature. 2010; 467:1114–17. [PubMed: 20981102]
18. Ambrus JL, Ambrus CM, Mink IB, Pickren JW. Causes of death in cancer patients. J Med. 1975; 6:61–64. [PubMed: 1056415]
19. Duda DG, Duyverman AM, Kohno M, Snuderl M, Steller EJ, Fukumura D, et al. Malignant cells facilitate lung metastasis by bringing their own soil. Proc Natl Acad Sci U S A. 107:21677–82. [PubMed: 21098274]
20. Hanley JA, McNeil BJ. The meaning and use of the area under a receiver operating characteristic (ROC) curve. Radiology. 1982; 143:29–36. [PubMed: 7063747]
21. Jiang P, Li X, Thompson CB, Huang Z, Araiza F, Osgood R, et al. Effective targeting of the tumor microenvironment for cancer therapy. Anticancer Res. 2012; 32:1203–12. [PubMed: 22493350]
22. Jacobetz MA, Chan DS, Neesse A, Bapiro TE, Cook N, Frese KK, et al. Hyaluronan impairs vascular function and drug delivery in a mouse model of pancreatic cancer. Gut. 62:112–20. [PubMed: 22466618]
23. Slidell MB, Chang DC, Cameron JL, Wolfgang C, Herman JM, Schulick RD, et al. Impact of total lymph node count and lymph node ratio on staging and survival after pancreatectomy for pancreatic adenocarcinoma: a large, population-based analysis. Ann Surg Oncol. 2008; 15:165–74. [PubMed: 17896141]
24. Erkan M, Michalski CW, Rieder S, Reiser-Erkan C, Abiatari I, Kolb A, et al. The activated stroma index is a novel and independent prognostic marker in pancreatic ductal adenocarcinoma. Clin Gastroenterol Hepatol. 2008; 6:1155–61. [PubMed: 18639493]
25. Apte MV, Haber PS, Darby SJ, Rodgers SC, McCaughan GW, Korsten MA, et al. Pancreatic stellate cells are activated by proinflammatory cytokines: implications for pancreatic fibrogenesis. Gut. 1999; 44:534–41. [PubMed: 10075961]
26. Theocharis AD, Tsara ME, Papageorgacopoulou N, Karavias DD, Theocharis DA. Pancreatic carcinoma is characterized by elevated content of hyaluronan and chondroitin sulfate with altered disaccharide composition. Biochim Biophys Acta. 2000; 1502:201–06. [PubMed: 11040445]
27. Anttila MA, Tammi RH, Tammi MI, Syrjanen KJ, Saarikoski SV, Kosma VM. High levels of stromal hyaluronan predict poor disease outcome in epithelial ovarian cancer. Cancer Res. 2000; 60:150–55. [PubMed: 10646867]
28. Auvinen P, Tammi R, Parkkinen J, Tammi M, Agren U, Johansson R, et al. Hyaluronan in peritumoral stroma and malignant cells associates with breast cancer spreading and predicts survival. Am J Pathol. 2000; 156:529–36. [PubMed: 10666382]
29. Setala LP, Tammi MI, Tammi RH, Eskelinen MJ, Lipponen PK, Agren UM, et al. Hyaluronan expression in gastric cancer cells is associated with local and nodal spread and reduced survival rate. Br J Cancer. 1999; 79:1133–38. [PubMed: 10098747]
30. Whatcott CJ, Han H, Posner RG, Hostetter G, Von Hoff DD. Targeting the tumor microenvironment in cancer: why hyaluronidase deserves a second look. Cancer Discov. 2011; 1:291–96. [PubMed: 22053288]
31. Linder S, Castanos-Velez E, von Rosen A, Biberfeld P. Immunohistochemical expression of extracellular matrix proteins and adhesion molecules in pancreatic carcinoma. Hepatogastroenterology. 2001; 48:1321–27. [PubMed: 11677955]
32. Grzesiak JJ, Ho JC, Moossa AR, Bouvet M. The integrin-extracellular matrix axis in pancreatic cancer. Pancreas. 2007; 35:293–01. [PubMed: 18090233]
33. Guo W, Giancotti FG. Integrin signalling during tumour progression. Nat Rev Mol Cell Biol. 2004; 5:816–26. [PubMed: 15459662]

34. Magzoub M, Jin S, Verkman AS. Enhanced macromolecule diffusion deep in tumors after enzymatic digestion of extracellular matrix collagen and its associated proteoglycan decorin. FASEB J. 2008; 22:276–84. [PubMed: 17761521]

35. Matsuda Y, Hagio M, Naito Z, Ishiwata T. Clinicopathological features of 30 autopsy cases of pancreatic carcinoma. J Nippon Med Sch. 2012; 79:459–67. [PubMed: 23291845]

Statement of Translational Relevance

Pancreatic desmoplasia is thought to impede proper drug delivery in pancreatic ductal adenocarcinoma therapeutic interventions. While desmoplasia in primary tumors has been studied, the presence or absence of desmoplasia at metastatic sites has not been investigated. The present study examines extracellular matrix deposition in sections from clinical samples of both primary pancreatic tumors and from various sites of metastasis. Based on Collagen I levels, our findings indicate that primary tumors and metastatic lesions show comparable levels of desmoplasia. Our findings also indicate a negative correlation between patient survival and extracellular matrix (Collagen I or Hyaluronan) deposition. As stromal targeting has gained traction as a potential approach to enhancing chemotherapeutic interventions, our analysis provides further support for use of the approach, even in patients with late stage, metastatic disease.

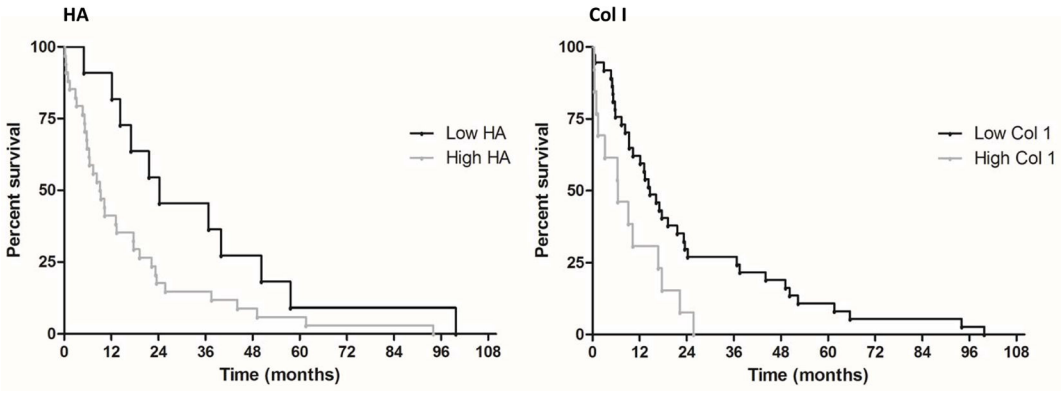

Figure 1.

Kaplan-Meier survival curves for patients with high and low levels of hyaluronan (HA) and Collagen I (Col I) in their primary tumors. Average staining positivity for HA in patient tissues was plotted in Kaplan-Meier curves which allowed us to compare ‘low’ and ‘high’ HA level groups. Median survival in the ‘high’ HA group was 9.3 months, as opposed to 24.3 months for the ‘low’ HA group. This difference amounted to a separation of 15.0 months in median survival between the ‘low’ HA and ‘high’ HA groups. Median survival in the ‘high’ Col I group was 6.4 months, as opposed to 14.6 months for the ‘low’ Col I group. The median difference was 8.2 months.

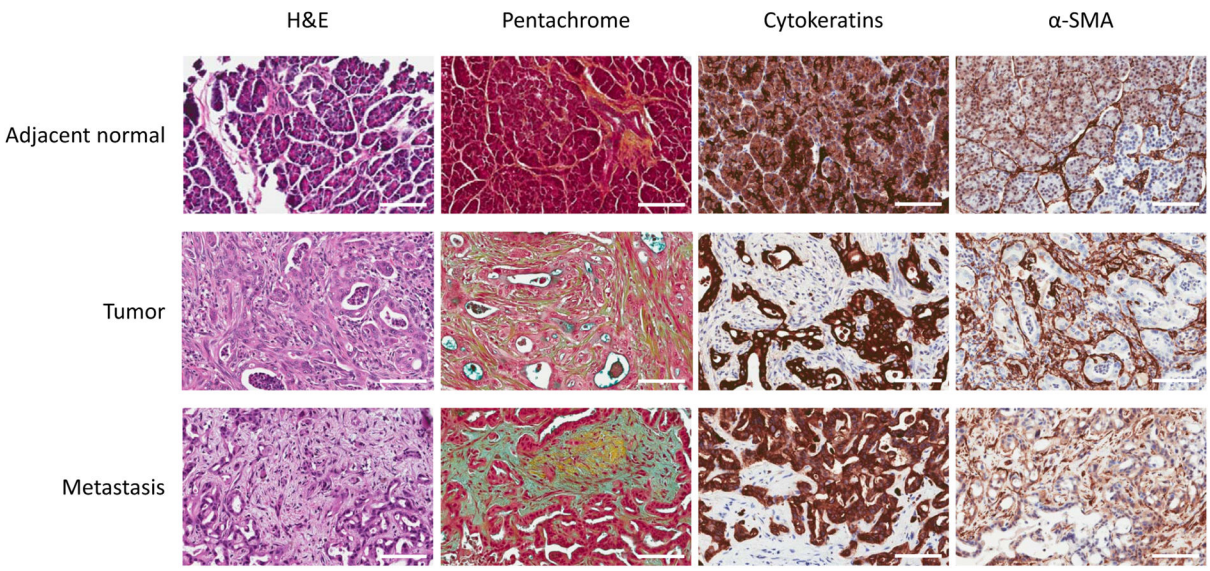

Figure 2.

Histochemical staining for stromal content of adjacent normal, primary tumor, and metastatic lesions. Representative images are shown of patient tissue sections stained by both standard H&E and Movat's pentachrome staining techniques. Representative images of cytokeratin and α-smooth muscle actin staining are also shown. Significant desmoplasia is seen in both tumor and liver metastases, but not in adjacent normal tissues. (Scale bar=100μm)

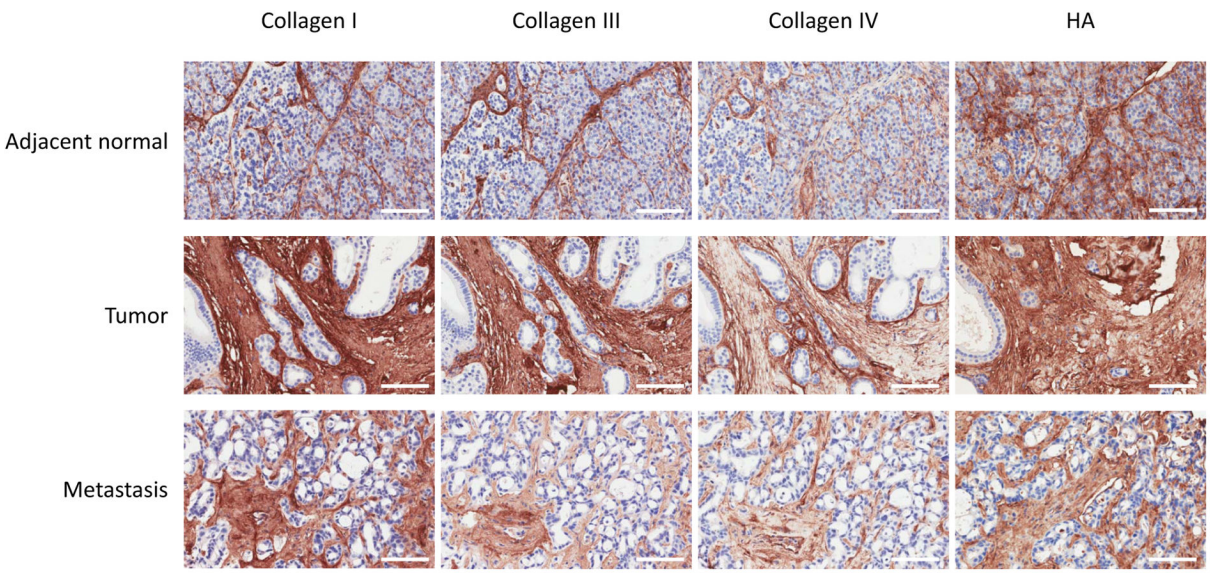

Figure 3.

Immunohistochemical assessment of collagen and HA expression in PDAC tissues. Patient tissues sections were stained with antibodies for Collagens I, III, IV, and HA. Representative images are shown of adjacent normal, primary tumor, and metastatic lesions. (Scale bar=100μm)

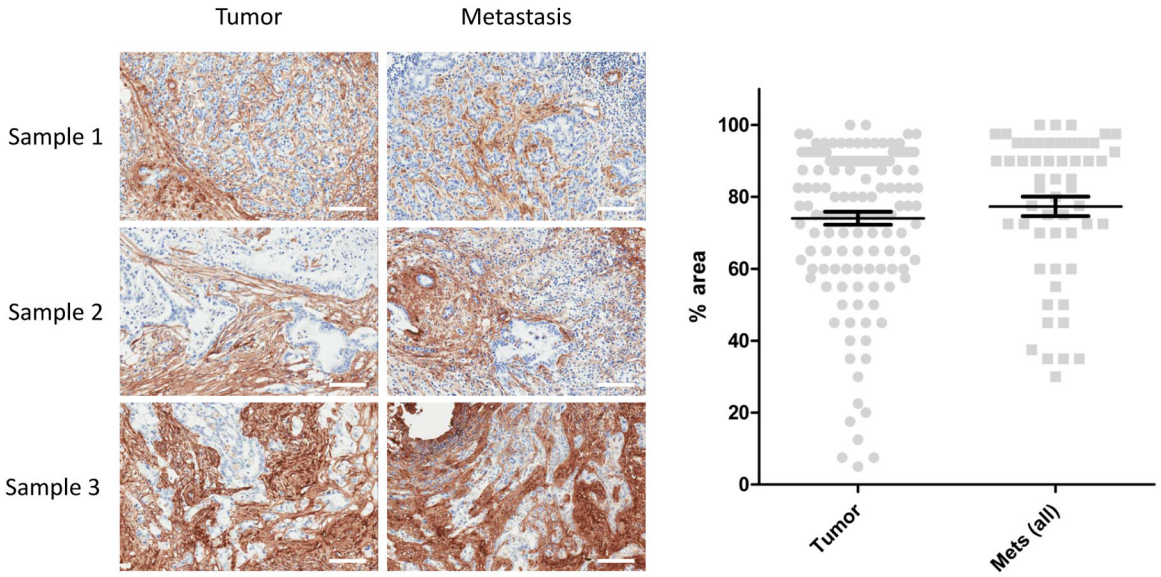

Figure 4.

Representative images of patient matched pancreatic primary and metastatic lesions stained for Collagen I, and quantitative assessment of stromal content of all primary tumors and metastatic lesions. Patient tissue sections (left panel) from confirmed cases of ductal adenocarcinoma were stained for Collagen I. Tumors and their matched metastatic lesions from three patients are displayed. Primary tumors and metastatic lesions show similar levels of Collagen I staining. Metastatic lesions shown were excised from the lymph node (sample 1), liver (sample 2), and mesentery (sample 3). (Scale bar=100μm) For comparison, sample scoring is shown in Table 2 (corresponding to samples 2, 3, and 4). In our quantitative assessment (right panel), the percent area of positive Collagen I staining was plotted for each case and grouped into primary tumor and metastases for comparison.

Table 1

Breakdown of metastatic lesions, by site

Site of metastasis	Cases	% total
Liver	26	46
Lung	3	5
Lymph node	7	12
Other	21	37

Table 2

Comparison of Col I staining in matched samples

Sample	Site	Pathology	% Area Col I	Intensity	Total score
1	Pancreas	Ductal adenocarcinoma, moderately differentiated	38.3	3	114.9
	Lung	Adenocarcinoma	10.2	3	30.7
2	Pancreas	Ductal adenocarcinoma, well differentiated	23.4	3	70.3
	Lymph node	Metastatic adenocarcinoma	11.5	3	34.6
3	Pancreas	Ductal adenocarcinoma, well differentiated	17.6	3	52.7
	Liver	Metastatic adenocarcinoma	18.0	3	54.1
4	Pancreas	Ductal adenocarcinoma, moderately differentiated	46.5	3	139.5
	Mesentery	Adenocarcinoma	53.8	3	161.5
5	Pancreas	Ductal adenocarcinoma, moderately differentiated	31.4	3	94.3
	Lymph node	Metastatic adenocarcinoma	26.6	3	79.7
6	Pancreas	Ductal adenocarcinoma, moderately differentiated	68.1	3	204.2
	Umbilicus	Metastatic adenocarcinoma	54.2	3	162.6
7	Pancreas	Adenocarcinoma, unspecified	35.1	3	105.4
	Liver	Metastatic adenocarcinoma	44.2	3	132.6